

# EVALUATION OF NEUTRON RESONANCE PARAMETERS FOR 19 FISSION PRODUCTS

Soo-Youl Oh and Jonghwa Chang  
Nuclear Data Evaluation Lab., Korea Atomic Energy Research Institute  
P.O.Box 105, Yusung, Taejon 305-600, Korea  
syoh@kaeri.re.kr, jhchang@kaeri.re.kr

Said F. Mughabghab  
National Nuclear Data Center, Brookhaven National Laboratory  
P.O.Box 5000, Upton, NY 11973-5000, U.S.A.  
mugabgab@bnlnd2.dne.bnl.gov

## ABSTRACT

The neutron resonance parameters for 19 fission product nuclides, important in the storage of spent fuel, transmutation study, and development of advanced fuel, have been evaluated. These are  $^{95}\text{Mo}$ ,  $^{99}\text{Tc}$ ,  $^{101}\text{Ru}$ ,  $^{103}\text{Rh}$ ,  $^{105}\text{Pd}$ ,  $^{109}\text{Ag}$ ,  $^{131}\text{Xe}$ ,  $^{133}\text{Cs}$ ,  $^{141}\text{Pr}$ ,  $^{143,145}\text{Nd}$ ,  $^{147,149-152}\text{Sm}$ ,  $^{153}\text{Eu}$ , and  $^{155, 157}\text{Gd}$ . Recent measurements of thermal cross sections and resolved resonance parameters, as well as previous neutron data reported in the BNL-325 compilations, were incorporated into new evaluations. The distributions of s- and, if known, p-wave neutron widths of resolved resonances were analyzed in terms of the Porter-Thomas distribution. The resulting neutron strength functions and average level spacings, thus determined, were applied in the evaluation of the unresolved energy region. The capture cross sections, calculated with the present evaluated parameters, are in better agreement with measurements than the corresponding ENDF/B-VI evaluations. The present evaluations are reviewed by CSEWG for consideration as candidates for new releases of ENDF/B-VI.

## 1. INTRODUCTION

In nuclear engineering dealing with the storage and transmutation of long-lived isotopes of spent fuel, neutron cross section data for fission product nuclides are of significant importance. Furthermore, in applied and basic research, such as the development of advanced fuel and astrophysical modeling, accurate knowledge of the neutron capture cross sections is a necessary ingredient for the success of such project. However, the latest release of ENDF/B-VI shows that most of the resonance parameter files for the major fission products are based on old measurements, some of which date back 20 years. Although recent libraries such as JEF-2.2 and JENDL-3.2 adopted recent measurements, major portions of the evaluations adopted Mughabghab's evaluated resonance parameters, as reported in the BNL compilations, published in 1981 and 1984<sup>1,2</sup>. Therefore, there is a compelling need for new evaluations which will incorporate the recent measurements. In the present evaluations, old data are also considered by renormalizing to the new standard cross sections.

The fission products selected in this evaluation are stable or long-lived (the shortest one is  $^{149}\text{Sm}$  of which half-life is 90 years) isotopes and largely contribute to the total neutron absorption in a system<sup>3</sup>. Even

though the importance of each nuclide depends more or less on the characteristics of a system such as the energy spectrum, the present evaluation covers almost all nuclides, except ones shortly decayed out, that should be dealt with explicitly in a neutronic calculation. We have evaluated the thermal cross sections and resonance parameters in the resolved and unresolved resonance energy regions. In addition, we established a systematic and computerized evaluation procedure during the course of this work.

## 2. EVALUATION METHODS

### 2.1 Resolved Resonance Region

In the resolved resonance region, we adopted the multi-level Breit-Wigner formalism. The resonance energy, orbital angular momentum of the incident neutron ( $l$ ), the resonance spin ( $J$ ), the neutron scattering width ( $\Gamma_n$ ), and the radiative width ( $\Gamma_\gamma$ ) are provided for each resonance.

The BNL compilations<sup>1,2</sup> were adopted as the primary sources for the resolved resonance parameters and thermal cross sections at 0.0253 eV. Subsequently, the recommended values in the compilations<sup>1,2</sup> were revised and/or supplemented by taking into account recent measurements. The old measurements were revisited by normalizing to the recent standards or corrected, if necessary. In the next step, one or two bound levels were invoked, if necessary, to reproduce the reference thermal cross sections and scattering lengths.

For a resonance with unknown  $l$  value, the Bayesian approach<sup>1</sup> was applied to calculate the probability that a resonance with a neutron width of  $g\Gamma_n$  is due to a p-wave ( $l=1$ ) neutron. Adopting the Porter-Thomas distribution<sup>4</sup> as a probability density function for reduced neutron widths and assuming the  $(2J+1)$  dependence of the level density, the probability is derived as follows:

$$P(p | g\Gamma_n) = \left[ 1 + \frac{1}{\beta} \frac{\sqrt{\frac{S_1 P_1}{S_0 P_0}} \exp\left\{ \frac{g\Gamma_n}{2\langle D_0 \rangle \sqrt{E}} \left( \frac{1}{S_1 P_1} - \frac{1}{S_0 P_0} \right) \right\}}{\alpha + (1-\alpha) \sqrt{\frac{\pi g\Gamma_n}{2\sqrt{E} \langle D_0 \rangle S_1 P_1}}} \right]^{-1},$$

where  $\langle D_0 \rangle$  is the s-wave average level spacing,  $S_0$  and  $S_1$  are the s- and p- wave neutron strength functions, respectively,  $E$  the resonance energy in eV, and  $P_0$  and  $P_1$  the s- and p-wave penetrabilities, respectively. The values of  $\alpha$  and  $\beta$  are given, respectively, as 1 and 3 for spin  $I = 0$  target nuclide,  $2/3$  and  $9/4$  for  $I = 1/2$ , and  $1/2$  and  $2$  for  $I \geq 1$ . If the calculated probability of a resonance is larger than a certain value, which was arbitrarily set to 0.5 in the present study, then the resonance is assigned as a p-wave resonance; otherwise, it is considered as a s-wave resonance. However, when the  $l$  value of a resonance is determined from measurements, the value is not modified regardless of the calculated probability. Meanwhile, the spins of resonances without measured  $J$  value are randomly assigned according to the  $(2J+1)$  dependence of the level density.

Finally, the distribution of reduced neutron widths was analyzed in terms of the Porter-Thomas distribution. With a stipulated cutoff value for the reduced neutron width, which excludes weak resonances from the analysis to reduce the effect of presumably missed weak resonances, a fit of the distribution of measured widths to the theoretical distribution yields the average level spacing and neutron strength function. This fitting provides good estimates for the average parameters for s-wave resonances but generally not for p- and d-wave resonances because of lack of assigned  $l$ -values. We have developed a

computer program that assigns  $l$  and  $J$  values applying the above methods and subsequently performs the fitting procedure to obtain average parameters.

## 2.2 Unresolved Resonance Region

The unresolved resonance region was stipulated to cover an energy range from the upper energy of the resolved region up to the first excited level for inelastic scattering. For most fission product isotopes under consideration, the inelastic channels are in the range of 50 ~ 200 keV. The present evaluation provides average resonance parameters for s-, p- and d-wave resonances. In principle, we adopted those average parameters which were obtained from the analyses of resolved resonances. The systematics of average parameters, described in the introduction of references 1 and 2, were considered as a guide in the evaluation process.

The Bethe's level density formula was adopted to calculate the energy-dependence of the level spacing in the unresolved energy region:

$$1/D(U, J) \propto \frac{(2J+1)}{U^{5/4}} \exp(2\sqrt{aU}) \exp\left\{-\frac{(J+1/2)^2}{2\sigma^2}\right\},$$

where  $U$  is the effective excitation energy which depends on the incident neutron energy,  $a$  the level density parameter, and  $\sigma$  the spin cutoff factor. Values of  $\sigma$ ,  $a$ , and other parameters for calculating  $U$  were adopted from references 5 and 6. The proportional constant was determined from the s-wave average level spacing determined in the resolved energy region.

Because of lack of measurements, the d-wave strength functions, as well as p-wave strength functions for some isotopes, were adopted from mass-dependent systematics<sup>1,2</sup>. The average radiative widths for p- and d-wave resonances were assumed to be equal to that of the s-wave resonances. In some cases, however, the average width for the p-wave component was adopted from systematics<sup>2</sup> or directly from the measurements (<sup>95</sup>Mo case). In some cases, the average parameters for high  $l$ -value resonances were adjusted to reproduce the measured capture cross sections in the unresolved energy region.

## 3. RESULTS AND DISCUSSIONS

The energy ranges of resonance region and number of resonances of the present evaluation are summarized in Table I and are compared with those in the ENDF/B-VI. In general, as shown in columns 5 and 6, many more resolved resonances are contained in the present evaluation than in the ENDF/B-VI. In addition, as shown in columns 7 and 8, the average parameters for the unresolved region were provided for all the isotopes under consideration, while the ENDF/B-VI does not provide unresolved resonance parameters for <sup>95</sup>Mo, <sup>105</sup>Pd, <sup>109</sup>Ag, <sup>131</sup>Xe, <sup>133</sup>Cs, <sup>141</sup>Pr, and <sup>151</sup>Sm.

Tables II and III show comparisons between the present evaluations and other evaluations for the 2200 m/s capture cross sections and capture resonance integrals, respectively. There are significant differences between the present evaluations and those in ENDF/B-VI for the capture cross sections of <sup>145</sup>Nd and <sup>147</sup>Sm, as well as for the resonance integrals of <sup>131</sup>Xe, <sup>133</sup>Cs, <sup>149</sup>Sm, and <sup>153</sup>Eu.

The average capture cross sections weighted with Maxwellian spectrum which is peaked at 30 keV were calculated for the present and ENDF/B-VI evaluations and are shown respectively in columns 6 and 5 of Table IV. For this comparison, point-wise cross sections of the ENDF/B-VI in the energy region from the upper energy limit of the present unresolved region to 1 MeV were adopted. In addition, comparisons

with other compilations and measurements are included in Table IV. For several isotopes, large differences between values from the present and ENDF/B-VI evaluations are observed; especially in the cases of  $^{143}\text{Nd}$  and  $^{149}\text{Sm}$ , significant improvements are shown by comparing with the recent measurements of Wisshak *et al.*<sup>13,14</sup>

Figure 1 shows the s-wave neutron strength functions. The data denoted by RIPL are taken from reference 17, and the line is the result of deformed optical model calculation<sup>2</sup>. The present values show reasonable agreement with those from various sources. For the calculation of average reduced widths in the unresolved region, the strength functions derived from the Porter-Thomas analysis were used. For  $^{105}\text{Pd}$  and  $^{109}\text{Ag}$ , as exceptional cases, the s-wave strength functions from the Porter-Thomas analysis were adjusted to reproduce measured capture cross sections at the low energy region.

In the unresolved resonance region, comparisons of the present capture cross sections with those from the ENDF/B-VI show improved capture cross sections. As an example, Figure 2 shows such improvement for the  $^{157}\text{Gd}$  case. It is worth noting that the s-wave (and p-wave for some isotopes) strength function and level spacing, determined from the Porter-Thomas analysis, are capable in predicting reliable capture cross sections in the unresolved resonance region.

#### 4. CONCLUDING REMARKS

We have considered all available measured data in the present evaluation in the thermal, resolved and unresolved energy regions. The present resonance parameters give a better description of the experimental data than those in existing libraries. In addition, the evaluation methods and physics models developed during this work can be used for future evaluations. We have proposed to the Cross Section Evaluation Working Group to adopt the present evaluations for the current release of the ENDF/B-VI.

#### ACKNOWLEDGEMENT

The Korea Ministry of Science and Technology has supported this work as one of its long-term nuclear R&D programs.

## REFERENCES

1. Mughabghab, S.F. *et al.*, *Neutron Cross Sections*, Vol.1, Part A, Academic Press, 1981.
2. Mughabghab, S.F., *Neutron Cross Sections*, Vol.1, Part B, Academic Press, 1984.
3. For instance, Takano, H. *et al.*, *Nucl. Technol.* **80**, 250, 1988.
4. Porter, C.E. and Thomas, R.G., *Phys. Rev.* **104**, 483, 1956.
5. Mughabghab, S.F. and Dunford, C.L., "New Approach for the Determination of the Nuclear Level Density Parameters," *Proc. Int'l Conf. on Phys. of Nucl. Sci. Technol.*, p.784, Long Island, U.S.A., Oct. 5-8, 1998.
6. Mughabghab, S.F. and Dunford, C.L., *Phys. Rev. Lett.* **81**, 4083, 1998.
7. Holden, N.E., "Neutron Scattering and Absorption Properties," *CRC Handbook of Chemistry and Physics*, 78<sup>th</sup> ed., CRC Press, 1998.
8. "Table of Simple Integral Neutron Cross Section Data from JEF-2.2, ENDF/B-VI, JENDL-3.2, BROND-2 and CENDL-2," JEF Report 14, OECD/NEA, Paris, 1994.
9. Abagyan, L.P., "The LIPAR-5 Resonance Parameter Library," INDC(CCP)-406, 1997.
10. Beer, H., Voss, F. and Winters, R.R., *Astrophys. J. Suppl. Ser.* **80**, 403, 1992.
11. Bao, Z.Y. and Kaeppler, F., *Atomic Data and Nucl. Data Tables* **36**, 411, 1987.
12. Ratynski, W. and Kaeppler, F., *Phys. Rev.* **C37**, 595, 1988.
13. Wisshak, K. *et al.*, *Phys. Rev.* **C57**, 391, 1998.
14. Wisshak, K. *et al.*, *Phys. Rev.* **C48**, 1401, 1993.
15. Toukan, K.A. *et al.*, *Phys. Rev.* **C51**, 1540, 1995.
16. Wisshak, K. *et al.*, *Phys. Rev.* **C52**, 2762, 1995.
17. Reffo, G., "Average Neutron Resonance Parameters," IAEA-TECDOC-1034, p.25, 1998.

Table I. Status of Resonance Data

Isotope	1st Inelastic Excited Level (keV) <sup>a</sup>	Upper Energy of RRR (keV)		No. of Resolved Resonances <sup>b</sup>		Upper Energy of URR (keV)	
		ENDF/B-VI	Present	ENDF/B-VI	Present	ENDF/B-VI	Present
42-Mo-95	204.12	2.188	2.141	25+ 30 (0)	20+ 35 (1)	–	206.3
43-Tc-99	140.51	0.800	0.983	42+ 25 (1)	41+ 54 (1)	141.4	141.9
44-Ru-101	127.23	1.000	1.035	40+ 0 (0)	41+ 7 (0)	100.0	128.5
45-Rh-103	39.756	1.500	4.116	59+ 60 (0)	101+178 (1)	40.4	40.2
46-Pd-105	280.51	1.000	2.054	80+ 0 (1)	141+ 57 (2)	–	283.2
47-Ag-109	88.034	2.509	4.996	83+ 0 (0)	236+ 71 (0)	–	88.8
54-Xe-131	80.185	4.000	3.945	39+ 0 (1)	45+ 2 (1)	–	80.8
55-Cs-133	80.997	2.500	3.989	123+ 0 (0)	148+ 39 (2)	–	81.6
59-Pr-141	145.44	0.991	10.049	15+ 0 (0)	79+ 47 (2)	–	146.5
60-Nd-143	742.05	5.285	5.503	121+ 27 (1)	122+ 27 (1)	100.0	225.0
60-Nd-145	67.220	4.140	3.979	212+ 0 (1)	194+ 0 (1)	50.0	67.7
62-Sm-147	121.22	1.000	1.998	140+ 0 (1)	211+ 0 (1)	30.0	122.1
62-Sm-149	22.507	0.100 <sup>c</sup>	0.520	29+ 0 (1)	158+ 0 (1)	10.0	100.0 <sup>d</sup>
62-Sm-150	333.86	1.600	1.563	22+ 0 (1)	22+ 0 (1)	100.0	336.1
62-Sm-151	4.821	0.300	0.296	120+ 0 (1)	120+ 0 (1)	–	66.2 <sup>e</sup>
62-Sm-152	121.78	5.025	5.102	91+ 0 (1)	91+ 0 (1)	100.0	122.6
63-Eu-153	83.367	0.097	0.098	71+ 0 (1)	71+ 0 (1)	1.0	83.9
64-Gd-155	60.009	0.183	0.183	92+ 0 (0)	92+ 0 (0)	10.4	60.4
64-Gd-157	54.533	0.307	0.307	56+ 0 (0)	60+ 0 (0)	10.4	54.9

a: In the center-of-mass system

b: Number of s-wave positive-energy resonances + Number of p-wave resonances; Number of bound level resonances in parentheses

c: Lower limit of the resolved resonance region (RRR) is 2.361 eV.

d: The second inelastic level is 277.075 keV in the center-of-mass system. e: This corresponds to the second inelastic level.

Table II. Capture Cross Sections at 0.0253 eV (barn)

Isotope	BNL Compilation	98CRC <sup>7</sup>	ENDF/B-VI <sup>a</sup>	JEF-2.2 <sup>a</sup>	JENDL-3.2 <sup>b</sup>	LIPAR-5 <sup>9</sup>	Present <sup>c</sup>	Relative Diff. (%) <sup>d</sup>
42-Mo-95	14.0±0.5	13.4±0.3	14.6	14.0	14.0	–	13.6	–7.4
43-Tc-99	20±1	23±2	19.6	19.1	19.6	–	20.0	2.0
44-Ru-101	3.4±0.9	5±1	3.43	3.42	3.36	–	3.45	0.6
45-Rh-103	145±2	145	147	146	147	–	145	–1.4
46-Pd-105	20.0±3.0	22±2	20.1	21.8	20.3	–	20.9	3.8
47-Ag-109	91.0±1.0	91.2	91.0	90.8	90.5	90.7	90.8	–0.2
54-Xe-131	85±10	90±10	90.6	85.1	85.0	–	90.0	–0.7
55-Cs-133	29.0±1.5	30.4	29.7	29.1	29.0	–	29.0	–2.4
59-Pr-141	11.5±0.3	11.5	11.5	11.5	11.5	–	11.5	0.0
60-Nd-143	325±10	330±10	325	323	330	319	325	0.0
60-Nd-145	42±2	47±6	42.1	41.9	43.8	41.9	49.8	15.5
62-Sm-147	57±3	56±4	57.5	57.2	58.0	56.7	50.0	–15.0
62-Sm-149	40140±600	40100±600	39730	40480	40150	39420	40530	2.0
62-Sm-150	104±4	102±5	104	103	109	108.2	100	–3.9
62-Sm-151	15200±300	15200±300	15250	15190	15160	15160	15170	–0.5
62-Sm-152	206±6	206±15	207	206	206	202	206	–0.5
63-Eu-153	312±7	300±20	313	300	313	312	312	0.0
64-Gd-155	60900±500	61000±1000	61100	60790	60890	60710	60730	–0.6
64-Gd-157	254000±815	254000±3000	255800	253400	254100	253500	253700	–0.8

a: Values taken from reference 8

b: From General Description (MF=1) of JENDL-3.2

c: Calculated using LINEAR–RECENT–SIGMA1–INTER codes

d: Relative Difference =  $(1 - \sigma_{\gamma}^{\text{ENDF/B-VI}} / \sigma_{\gamma}^{\text{Present}}) \times 100$

Table III. Capture Resonance Integrals (barn)

Isotope	BNL Compilation	98CRC <sup>7</sup>	ENDF/B-VI <sup>a</sup>	JEF-2.2 <sup>a</sup>	JENDL-3.2 <sup>b</sup>	LIPAR-5 <sup>9</sup> <sup>c</sup>	Present <sup>d</sup>	Relative Diff. (%) <sup>e</sup>
42-Mo-95	109±5	109±5	113	110	119	–	111	–2.2
43-Tc-99	340±20	–	350	304	312	–	312	–12.2
44-Ru-101	100±20	110±30	111	111	100	–	111	0.1
45-Rh-103	1100±50	1180	1035	1035	1040	–	1036	0.1
46-Pd-105	62.2	60±20	111	93.1	96.8	–	95.2	–16.6
47-Ag-109	1400±48	1480	1471	1473	1470	1467	1476	0.4
54-Xe-131	900±100	900±100	1016	890	900	–	882	–15.2
55-Cs-133	437±26	422	383	439	396	–	421	9.0
59-Pr-141	17.4±2.0	14±3	19.0	17.9	18.4	–	17.6	–7.7
60-Nd-143	128±30	128±30	130	130	130	127	130	0.7
60-Nd-145	240±35	260±40	231	231	204	228	245	5.7
62-Sm-147	–	710±50	789	794	781	721	777	–1.4
62-Sm-149	3390	3100±500	3258	3484	3490	3355	3482	6.4
62-Sm-150	358±50	290±30	338	339	325	334	334	–1.2
62-Sm-151	3520±160	3520±60	3449	3465	3410	3397	3430	–0.6
62-Sm-152	2970±100	3000±300	2981	2977	2770	2958	2976	–0.2
63-Eu-153	1420±100	1800±400	1499	1448	1410	1305	1408	–6.5
64-Gd-155	1447±100	1540±100	1555	1543	1540	1437	1537	–1.2
64-Gd-157	700±20	800±100	759	762	763	711	754	–0.7

a: Values taken from reference 8

b: From General Description (MF=1) of JENDL-3.2

c: Integrated from 0.5 eV to the upper energy of resolved resonance region

d: Calculated using LINEAR–RECENT–SIGMA1–INTER codes; Integrated from 0.5 eV to 100 keV with 1/E spectrum

e: Relative Difference =  $(1 - I_{\gamma}^{\text{ENDF/B-VI}} / I_{\gamma}^{\text{Present}}) \times 100$



Table IV. Average Capture Cross Sections Weighted with Maxwellian Spectrum Peaked at 30 keV (mb)

Isotope	Measured			Calculated <sup>a</sup>		
	Beer's Compilation <sup>10</sup>	Bao's Compilation <sup>11</sup>	Recent Data	ENDF/B-VI	Present	Relative Diff. (%)
Mo-95	292 ± 12	374 ± 50		375	377	0.4
Tc-99	782 ± 39	779 ± 40		855	795	-7.5
Ru-101	996 ± 40	996 ± 40		952	970	1.8
Rh-103	810 ± 14	875 ± 35		943	836	-12.7
Pd-105	1199 ± 60	1199 ± 60		1150	1190	3.3
Ag-109	779 ± 23	779 ± 23		807	787	-2.6
Xe-131	453 ± 81	348		291	306	5.1
Cs-133	509 ± 21	509 ± 21		552	513	-7.5
Pr-141	119 ± 15	119 ± 15		115	117	1.7
Nd-143	242 ± 10	253 ± 10 <sup>b</sup>	244.6 ± 3.1 <sup>13</sup>	287	239	-19.9
Nd-145	485 ± 100	485 ± 100	424.8 ± 4.5 <sup>13</sup>	444	423	-5.0
Sm-147	1005 ± 100	1005 ± 100	973.1 ± 10.0 <sup>14</sup>	931	929	-0.2
Sm-149	1409 ± 65	1454 ± 66	1819.9 ± 17.2 <sup>14</sup>	2384	1866	-27.8
Sm-150	434 ± 26	447 ± 26	421.9 ± 3.8 <sup>14</sup>	378	409	7.5
Sm-151	1932 ± 206	1932	1825 ± 450 <sup>c</sup>	2466	2569	4.0
Sm-152	401 ± 24	396 ± 22 <sup>b</sup>	473.2 ± 4.4 <sup>14</sup>	494	460	-7.4
Eu-153	3170 ± 317	3170 ± 317		2575	2486	-3.5
Gd-155	2721 ± 90	2800 ± 280	2648 ± 30 <sup>16</sup>	2592	2564	-1.1
Gd-157	1355 ± 39	1538 ± 154	1369 ± 15 <sup>16</sup>	1387	1361	-2.0

a: Using INTER; integrated from 10<sup>-5</sup> eV to 1 MeV and multiplied by 2/√π

b: Re-normalized value as reported in reference 12

c: Calculated value presented in reference 15

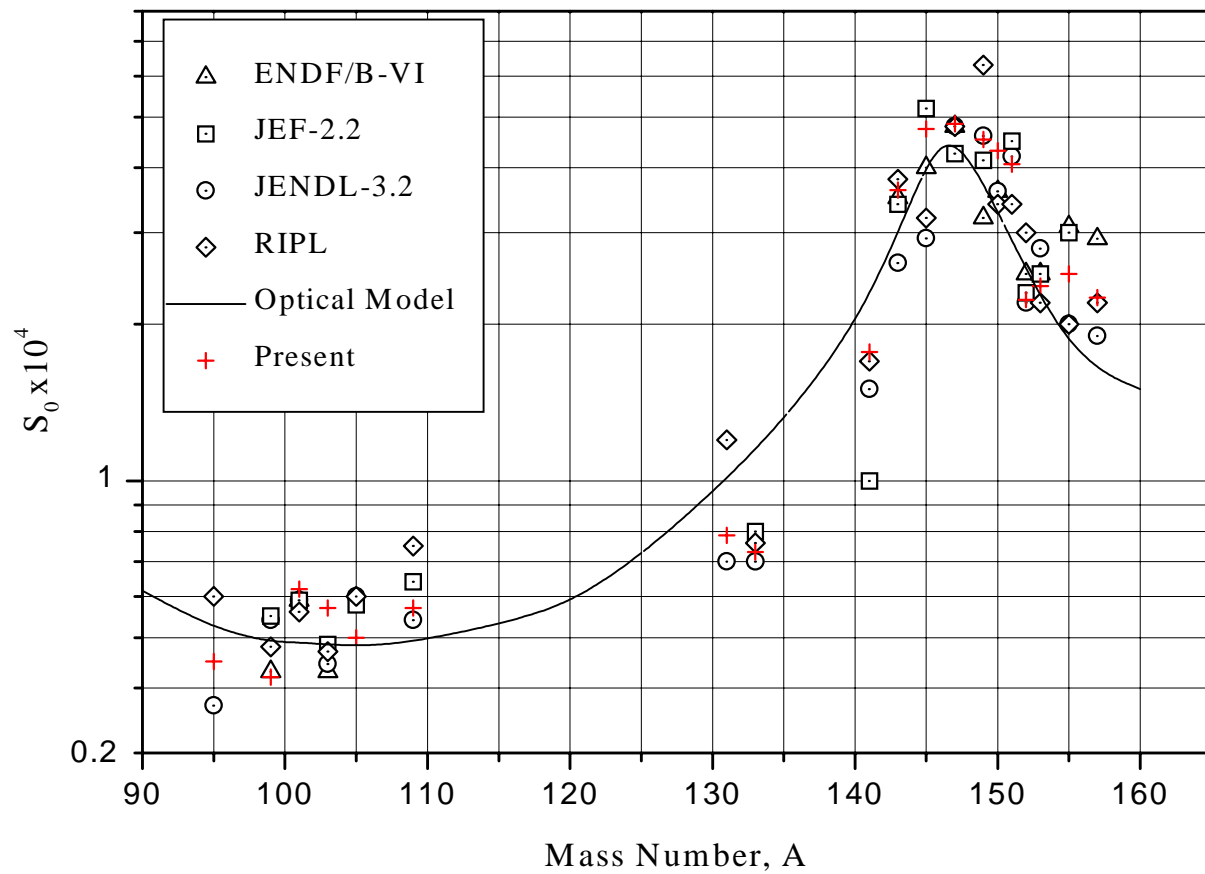


Figure 1. s-wave Neutron Strength Functions

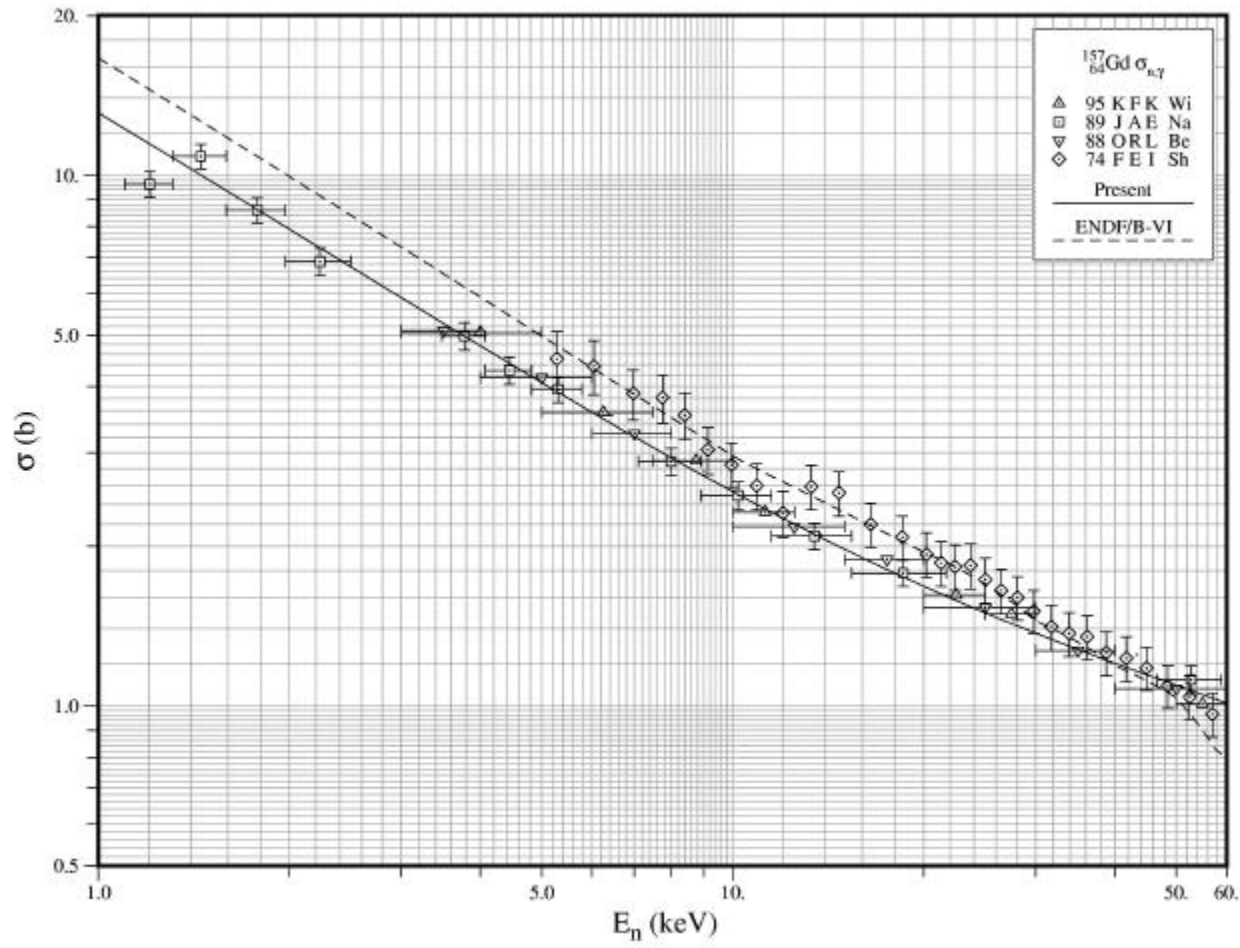


Figure 2. Comparison of Capture Cross Sections of  $^{157}\text{Gd}$  in keV Region